Temperature-Dependent Hydrogen Electrochemistry on Platinum Low-Index Single-Crystal Surfaces in Acid Solutions

N. M. Marković,* B. N. Grgur, and P. N. Ross

Materials Sciences Division, Lawrence Berkeley National Laboratory, University of California, Berkeley, California 94720

Received: March 12, 1997; In Final Form: May 4, 1997[⊗]

The hydrogen evolution (HER) and the hydrogen oxidation reaction (HOR) were studied on platinum single crystals in a sulfuric acid solution over the temperature range 274−333 K. We found, *for the first time*, that at a fixed temperature (274 K) the exchange current densities (i_o) increase in the order (111) ≪ (100) < (110), with the i_o on the (110) surface being 3 times that on the (111) surface. We also found that each crystal face has an unique, temperature-dependent Tafel slope for the HOR, and that the activation energies for the HER and the HOR decrease in the sequence $\Delta H^{\#}_{111} > \Delta H^{\#}_{100} > \Delta H^{\#}_{110}$, the same sequence as the order of activity. These differences in activation energy with crystal face are attributed to structure-sensitive heats of adsorption of the active intermediate, H_{ad}, whose physical state is unclear. We analyzed the kinetic data with a model for the coupling of this unknown state, H_{ad}, with the well-known adsorbed state of hydrogen, H_{upd}, whose adsorption energy is strongly structure-sensitive. We concluded that on Pt(110), the reaction follows the Tafel−Volmer mechanism with the Tafel (recombination) step rate determining. On Pt(100), the reaction follows the Heyrovsky−Volmer sequence, with the Heyrovsky (ion−atom) reaction step being the rate-determining step. The reaction mechanism on Pt(111) could not, however, be resolved by analyzing the kinetic parameters. The relatively low activity and high activation energy for the (111) surface is attributed to strong repulsive interaction between H_{ad} adatoms on this surface.

1. Introduction

The hydrogen evolution reaction (HER) and the hydrogen oxidation reaction (HOR) on a platinum electrode are among the most widely studied electrochemical reactions. It is nonetheless still unclear as to the sensitivity of these reactions to the microstructure of the Pt surface. Early kinetic studies of the HER and the HOR were carried out either on a polycrystalline platinum electrode[1] or on platinum single crystals that had poorly defined surface structures.[2,3] In 1970, Physnogreva *et al.*[2] and Scoulander *et al.*[3] reported that the kinetics of the HER on Pt(*hkl*) is not sensitive to the surface crystallography. In these experiments, however, the electrodes were "activated" and cleaned by cycling the electrode potential deep into the region of the oxide formation, a pretreatment which we now know disorders the surface. Only recently have the kinetics of the HER been studied on well-ordered platinum single-crystal electrodes[4−8] On the basis of potential step measurements, Seto *et al.*[6] reported that in perchloric acid, even on well-ordered Pt(*hkl*), the kinetics of the HER is insensitive to the crystallography of the surface. This was rather a surprising result, considering that the underpotential deposition of hydrogen, H_{upd}, the adsorbed state of hydrogen observed in cyclic voltammetry, is found to be strongly affected by the crystallographic orientation of the platinum surface atoms.[9] Seto *et al.*[6] also suggested that the invariance of the reaction rate reflects compensation between the differences in the standard Gibbs energy of hydrogen adsorption and the differences in the repulsive lateral interactions between adsorbed hydrogen adatoms on the different Pt(*hkl*) faces. The kinetic studies of the HER on Pt(*hkl*) with the rotating hanging meniscus electrode (RHME) by Kita *et al.*[7] also indicated that the HER is a structure-insensitive process in sulfuric acid. Given that the H_{upd} is strongly affected by the surface geometry, they proposed that H_{upd} is not an intermediate in the HER. Gomez *et al.*[8] has also found that the HER on platinum single crystals is independent of the crystallographic orientation. By examining the kinetics of the HER and the process of the formation of H_{upd} on the platinum single-crystals surface modified by bismuth and antimony adatoms, they agreed with the previous findings by Protopopoff and Marcus[4] (who used sulfur adatoms) that H_{upd} cannot be an intermediate in the HER. It should be noted that all of these studies[4−8] were conducted at a single temperature, nominally 298 K (or just ambient temperature).

In contrast to these results for the HER in acid solutions, we recently found that the kinetics of the HER and the HOR on Pt(*hkl*) in alkaline electrolytes varies with the crystal face.[5] The activity for the HER in alkaline solution increased in the sequence (111) < (100) < (110); a similar order of activities has been found for the HOR, *e.g.*, (111) ≈ (100) ≪ (110). These differences in activity with crystal face are attributed to different states of adsorbed hydrogen and to different effects of these states on the mechanism of the hydrogen reaction. As in the above cited studies in acid solution, we also concluded that the high binding energy state of adsorbed hydrogen, H_{upd}, is not an intermediate in the reaction and in fact is a spectator species and has a site-blocking effect on the rates of both the HER and HOR. The findings that the HER is a structurally insensitive reaction in acid solutions but structurally sensitive in base solution is actually a surprising result, giving that the mechanism of the HER on a polycrystalline platinum electrode in an acid solution is probably the same as in an alkaline solution.[5] We decided, therefore, to re-examine the kinetics of the HER and HOR in our own laboratory. We were concerned that due to the very fast kinetics of the HER in acid solution[10] it would be experimentally very difficult to correlate the rate of the reaction with the surface geometry, even if the kinetics were indeed

* Corresponding author. Address: Lawrence Berkeley Laboratory, Mail Stop 2-100, Berkeley, CA 94720. Phone: (510)-486-4793. FAX: (510)-486-5530.

[⊗] Abstract published in *Advance ACS Abstracts,* June 15, 1997.

S1089-5647(97)00930-9 CCC: $14.00

dependent on the crystallographic orientation of Pt(*hkl*). In order to circumvent this problem, *i.e.*, the fast kinetics of the HER in acid solutions *at room temperature*, as we did with alkaline solution, we measured the kinetics of these processes in acid solution at the lowest temperatures possible with dilute solutions, *e.g.*, 274 K.

In this paper, we utilized the rotating disk technique we have developed[11] for single-crystal Pt disk electrodes ($RD_{Pt(hkl)}E$) and present results for the kinetics of both the HER and the HOR in acid solution at 274−333 K. *For the first time*, a structural sensitivity of the kinetics of both the HER and HOR is seen on Pt(*hkl*) in 0.05 M H_2SO_4 solution with activation energies that vary with crystal face. There is, thus, a compensation effect which narrows the differences in rate between crystal faces at 298 K, which explains in part the absence of structure sensitivity in previous studies at ambient temperature. We present a detailed analysis of the kinetic parameters, including exchange current densities, Tafel slopes, and activation energies, and suggest the most probable reaction mechanisms for the HER and HOR on the different Pt(*hkl*) surfaces in dilute sulfuric acid solution.

2. Experimental Section

The pretreatment and assembling of the Pt(*hkl*) single crystals (0.283 cm^2) in a $RD_{Pt(hkl)}E$ configuration was fully described previously.[11] Following flame annealing, the single crystal was mounted in the disk position of an insertable ring disk electrode (RDE) assembly.[11] Subsequently, it was transferred into a standard electrochemical cell and immersed into 0.05 M H_2SO_4 (J. T. Baker reagent) under potentiostatics control at ≈0.2 V. The cleanliness of the transfer and the electrolyte, even under sustained rotation at high rotation rates, was demonstrated in our previous work.[11] Upon immersion, the electrolyte was equilibrated for 5 min with the hydrogen gas (Spectra Gases, 6 N). All experimental measurements reported in this study were conducted in a standard three-compartment electrochemical cell equipped with the water jacket. A circulating constant temperature bath (Fisher Isotemp Circulator) maintained the temperature of the electrolyte within ±0.5 °C. All measurements were conducted *nonisothermally*, *i.e.*, keeping the temperature of reference electrode constant (*ca.*, 298 K) while that of the working electrode is varied from 274 to 333 K. The reference electrode was a saturated calomel electrode separated by a bridge in order to prevent Cl^- contamination of electrolytes. However, all potentials were corrected to a "constant-temperature" scale, and are referenced to the reversible hydrogen electrode at 1 atm of hydrogen at the same temperature in the same electrolyte. Current−potential curves were obtained potentiodynamically (sweep rate 10 mV/s) and were recorded simultaneously on a chart recorder and digitally on an IBM PC (486) computer using Labview for Windows.

3. Results

3.1. Temperature Effects on Cyclic Voltammetry of Pt(*hkl*): Adsorption Isotherms. Figure 1 shows cyclic voltammograms for Pt(*hkl*) in 0.05 M H_2SO_4, recorded at 274, 303, and 333 K. It is obvious that voltammetric features for all three single crystals, recorded over the range of temperature studied, are very similar to those observed at a room temperature.[7,11] Given that consensus in interpretation appears to be emerging with respect to the nature of processes which occur on Pt(*hkl*) in a sulfuric acid solution at the ambient temperature, only a brief interpretation of the voltammograms recorded at 274 K will be presented in this section. The current−potential curve of Pt(111), Figure 1c, gives a distinctive voltammogram with a

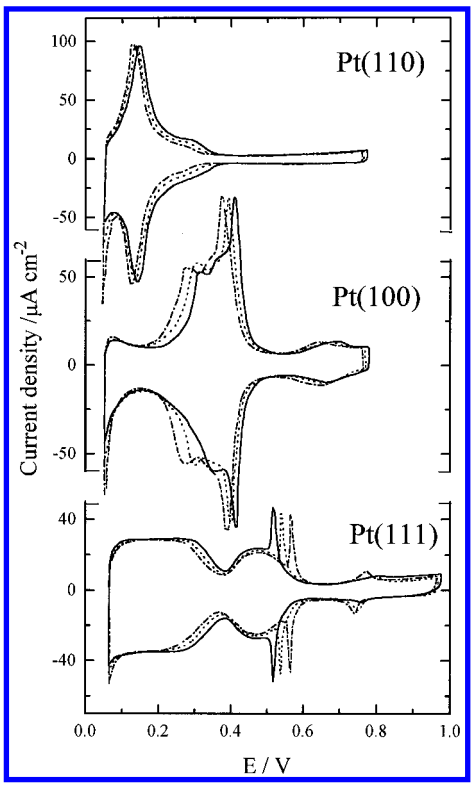

Figure 1. Cyclic voltammograms of Pt(*hkl*) in the $RD_{Pt(hkl)}E$ configuration in 0.05 M H_2SO_4 at (—) 274 K, (- - -) 303 K, and (— —) 333 K; rotation rate, 900 rpm; sweep rate, 50 mV/s.

broad, nearly flat hydrogen desorption/adsorption peak between ≈0.05 < *E* < 0.375 V, and the so-called "anomalous" peak at ≈0.4−0.6 V, which corresponds to the adsorption/desorption of bisulfate anions.[12] The main characteristic of the well-ordered Pt(100) voltammetry in sulfuric acid is that the two well-delineated peaks at 0.4 and 0.25 V correspond to the coupling of hydrogen adsorption with the bisulfate anion desorption on (100) terrace sites and *n*(100) × (111) step sites, respectively.[13] In the case of the Pt(110) surface in 0.5 M H_2SO_4, the initial adsorption of hydrogen, most likely at (111) microfacets (0.2 < *E* < 0.3 V), is followed by the adsorption of hydrogen at the step sites (0.05 < *E* < 0.2 V). The adsorption of hydrogen at the step sites, however, is accompanied by the desorption of bisulfate anions.[13]

For the sweep rate employed here, the underpotential deposition of hydrogen is at quasi-equilibrium, and the adsorption isotherm may be obtained directly by integration of the voltammetry curves shown in Figure 1. Again, because the shape of the adsorption isotherms as well as the charge associated with the hydrogen adsorption on Pt(*hkl*) were almost independent of the temperature of the electrolyte, only adsorption isotherms assessed for H_{upd} on Pt(*hkl*) at 274 K will be shown (see Figure 2). In this work, the fractional coverage for H_{upd}, $\theta_{H_{upd}}$, is based on the surface atomic density assuming one-electron transfer per surface atom. The surface atomic densities for (111) and (100) were based on their unreconstructed (1 × 1) geometry rather than any reconstructed phase, because our recent surface X-ray scattering (SXS) studies confirmed the (1 × 1) structure of the Pt(111) (1.5 × 10^{15} atoms/cm^2) and Pt(100) (1.3 × 10^{15} atoms/cm^2) single crystals in contact with several electrolytes.[14,15] SXS results for Pt(110) have indicated that Pt(110), prepared by the flame annealing−hydrogen cooling method, is reconstructed into a (1 × 2) structure with a surface density of 4.6 × 10^{14} atoms/cm^2.[15] The theoretical charge for the formation of the monolayer of H_{upd} on the (1 × 1) and (1 × 2) surfaces, however, is the same (≈147 μC/cm^2) since two

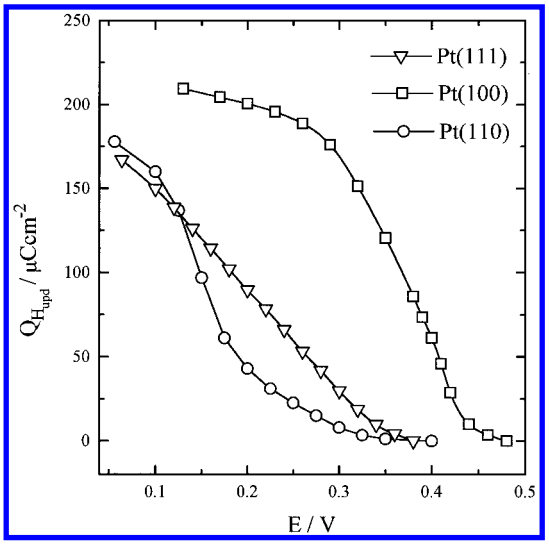

Figure 2. Plots of the charge associated with the underpotential deposition of hydrogen (H_{upd}) on Pt(*hkl*) in 0.05 M H_2SO_4 at 274 K.

H_{upd} adatoms can be adsorbed per unit cell of the reconstructed Pt(110)-(1 × 2) surface. The maximum charge associated with the underpotential deposition of hydrogen on the Pt(111) surface at 274 K is ≈160 μC/cm^2 (see Figure 2). The theoretical charge assuming one hydrogen atom for each surface platinum atom would be 240 μC/cm^2 for the Pt(111)-(1 × 1) surface, indicating that within the hydrogen underpotential deposition region the Pt(111) surface is covered only by 0.66 mL of the H_{upd}. Figure 2 also shows that on Pt(100) in the hydrogen adsorption region the absolute charge equals ≈225 μC/cm^2; note that the theoretical charge for 1 mL of H_{upd} on Pt(100) is 208 μC/cm^2. The difference between the experimental value and the theoretical charge, *ca.* 20 μC/cm^2, may be assigned to the charge from concomitant bisulfate adsorption/desorption in this potential region. In the case of Pt(110), the absolute charge evaluated by integration of the charge in the hydrogen adsorption region varied very little with temperature and equals ≈180 μC/cm^2; see Figure 2. The theoretical charge, assuming two hydrogen atoms adsorbed per unit cell of the reconstructed Pt(110)-(1 × 2), would be 147 μC/cm^2.[15] The difference between the experimental value and the theoretical charge, *ca.* 30 μC/cm^2, may be assigned to the charge from concomitant bisulfate adsorption/desorption process in this potential region.[13]

A detailed analysis of the temperature effects on the underpotential deposition of hydrogen on Pt(*hkl*) in sulfuric acid, *e.g.*, isosteric heats of adsorption, will be presented elsewhere. For our purposes here we should note that there are two characteristics of the voltammetric curves that represent the temperature effects. The first is that no new features are observed that would result from the temperature increase. The second characteristic is that on all single-crystal surfaces hydrogen adsorption/desorption peaks are shifted negatively by increasing the temperature. These observations have been reported by Zolfaghari *et al.* for the polycrystalline platinum electrode[16] and by Morin *et al.* for the Pt(100) electrode.[17] Cyclic voltammograms for the Pt(111) surface, Figure 1c, reveal that while the hydrogen adsorption curves are shifted negatively in potential by increasing the temperature from 274 to 333 K, the bisulfate adsorption/desorption peaks are shifted positively, confirming that the process associated with the "anomalous" feature is different from the underpotential deposition of hydrogen. A close inspection of Pt(100) and Pt(110) voltammograms indicates that by increasing the temperature from 274 to 333 K the voltammetric peaks in the potential region where hydrogen deposition is accompanied by bisulfate anion desorption are shifted negatively, as was the case of hydrogen adsorption on the Pt(111) surface free of bisulfate anions. This may imply that the changes observed in the hydrogen adsorption region on Pt(100) and Pt(110) are mostly driven by the enthalpy term for hydrogen adsorption and not by the weakly adsorbed bisulfate anions. Note that over the same temperature range the bisulfate adsorption on (111) is shifted positively by increasing the temperature.

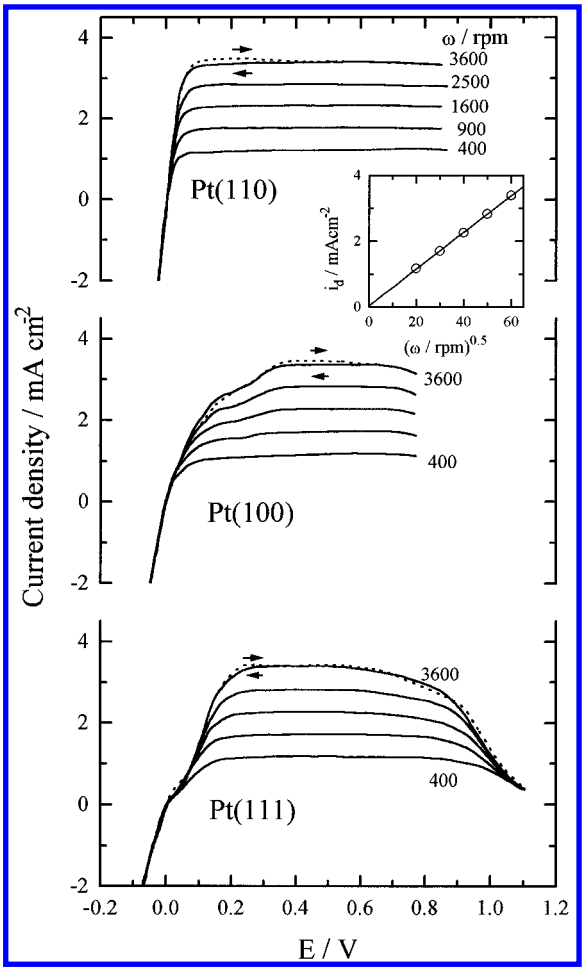

Figure 3. Polarization curves for the HER and the HOR on Pt(*hkl*) in 0.05 M H_2SO_4 at 274 K; sweep rate, 10 mV/s. Inset. i_d *versus* $\omega^{0.5}$ plot for the HOR on Pt(*hkl*) at 0.5 V.

3.2. Polarization Curves for the HER and the HOR on Pt(*hkl*). The HER and the HOR on Pt in acid electrolytes are among the fastest known electrochemical reactions, and it is experimentally very difficult to measure anything but diffusion polarization. It is our contention that, in order to illuminate the fine details of the hydrogen reaction and to establish the role of the Pt(*hkl*) surface geometry on the kinetics of the hydrogen reaction, the reaction rate of the HER and the HOR should be slowed down, *i.e.*, should be examined at the lowest temperature possible (274 K) in dilute solutions (0.05 M H_2SO_4). This, will in turn, enable us to extract true kinetic rates by use of the mathematically well-established correlation for the hydrodynamics of the RDE assembly. Although a complete set of the polarization curves were recorded in the temperature range 274−333 K (at intervals of 10 K), only representative curves will be shown and discussed.

3.2.1. Kinetics of the HER and the HOR on Pt(*hkl*) at 274 K. Polarization curves for the HER and the HOR at 1 atm of H_2 recorded on rotating Pt(*hkl*) disk electrodes in 0.05 M H_2SO_4 at 274 K are shown in Figure 3. For the HER, essentially no dependence of current density on the rotation rate was

observed on all three single-crystal surfaces. Very reproducible current *versus* potential relationships were established at a rotation rate as low as 900 rpm, indicating that at and above the rotation of 900 rpm the supersaturation effect by molecular H_2 is practically eliminated. It is very important to note that even at 274 K the exchange current density for the HER is still very high. Consequently, reliable Tafel slopes for the HER could not be determined on Pt(*hkl*) in 0.05 M H_2SO_4, since the measurements must be extended to rather high current densities where interference by uncompensated solution resistance and mass transport limitations can be significant.

The anodic polarization curves for the (110) surface are shown in Figure 3. A close inspection of Figure 3 reveals that at low overpotentials there is little or no rotation dependence of the hydrogen oxidation currents. Figure 3 also shows that the anodic current rises sharply from the origin and reaches the limiting current at overpotentials of *ca.* 60 mV. This indicates that the HOR on Pt(110) is kinetically controlled in a very narrow potential range and that hydrogen oxidation current densities, i, on Pt(110) are manly determined by diffusion overpotential, η_d, following closely the overpotential−current density relation[1a]

$$\eta_d = -\frac{RT}{2F}\ln\left(1-\frac{i}{i_d}\right) \qquad (1)$$

where i_d represents the measured diffusion-limited current at any given rotation rate. Thus, to obtain kinetic data for this surface, we must concentrate on analysis of the "micropolarization" potential region, as described below.

Above 0.4 V on all three surfaces, there appears to be well-defined diffusion-limiting currents, i_d. The theoretical value of i_d for an RDE is given[18]

$$i_d = 0.62nFD^{2/3}\nu^{-1/6}c_0\omega^{1/2} = Bc_0\omega^{1/2} \qquad (2)$$

where D is the diffusivity of hydrogen in 0.5 M H_2SO_4 ($D_{25\,°C} = 3.7 \times 10^{-5}$ cm^2/s, estimated from the product of H_2 diffusivity at infinite dilution and the ratio of the dynamic viscosities of the electrolyte and pure water), n is the number of electrons in the H_2 oxidation reaction (*i.e.*, $n = 2$), ν is the kinematic viscosity of the electrolyte ($\nu_{25\,°C} = 1.07 \times 10^{-2}$ cm^2/s), c_0 is the solubility of H_2 in 0.05 M H_2SO_4 ($c_{25\,°C} = 7.14 \times 10^{-3}$ M), and ω is the rotation rate. The calculated value of Bc_0 at 298 K is 6.54×10^{-2} (mA/cm^2)rpm$^{-1/2}$. The experimental values for i_d at 274 K at various rotation rates are plotted in the inset of Figure 3. The slope of this plot, which is the experimental value of Bc_0, is 5.6×10^{-2} (mA/cm^2)rpm$^{-1/2}$ at 274 K and 8.8×10^{-2} (mA/cm^2)rpm$^{-1/2}$ at 333 K, which are in reasonable agreement with the theoretical value at 298 K.

On the other hand, the polarization curves for Pt(111) reveal that up to about +0.05 V there is no rotation rate dependence, implying entirely kinetic resistance of the HOR. Sweeping the electrode potential more positively, the HOR is first under mixed kinetic-diffusion control, and above ≈+0.2 V well-defined diffusion-limiting currents are observed. It is interesting to note that a diffusion-limiting current for the HOR is still observed on Pt(111) in the 0.4−0.6 V potential region where there is adsorption by bisulfate anions, reportedly to very high coverages.[19] Above ≈0.85 V, however, the current decreases continuously up to ≈1.1 V, presumably due to the additional hydroxyl adsorption (see irreversible peaks at ≈0.75 V). It is also worth noting that Pt(111) is the least active surface, even though it is only one of the three surfaces on which there are no bisulfate anions specifically adsorbed in the low overpotential region.

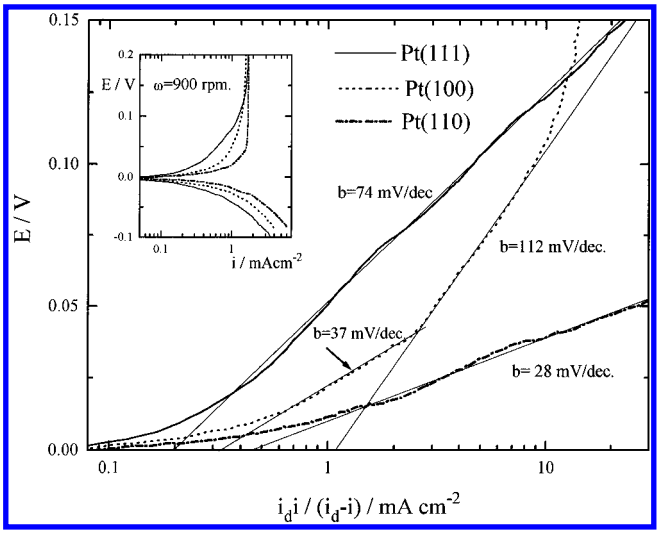

Figure 4. Tafel plots of mass transfer corrected currents for the HOR on Pt(*hkl*) in 0.05 M H_2SO_4 at 274 K. Inset. Polarization curves for the HER and HOR at low overpotentials; rotation rate, 900 rpm.

The anodic polarization curves for the (100) surface (Figure 3b) show that the kinetics of the HOR, initially under activation control, $\approx 0 < E < 0.05$ V, is followed by a region of mixed kinetic-diffusion control up to *ca.* 0.4 V, and above 0.4 V true diffusion-limiting currents are recorded. Qualitatively, this surface has a significantly higher activity than (111) but not as high as (110). Figure 3 also indicates that relative to the HER the HOR is under mixed diffusion-kinetic control over a wider range of potentials and provides the better opportunity for detailed kinetic analysis.

3.2.2. Tafel Plots. Figure 4 shows Tafel plots of mass transport corrected currents for the HOR at Pt(*hkl*) surfaces in 0.05 M H_2SO_4 at 274 K. The Tafel slopes are determined at low overpotentials, where measured current densities are essentially due to a mixed diffusion-kinetic resistance for the HOR. For Pt(110), we fitted the curves with one slope, ≈28 mV/dec with an exchange current density of $\approx 0.65 \times 10^{-3}$ A/cm. On Pt(100), the HER appears to have two Tafel slopes, at low overpotentials ≈37 mV/dec and at high overpotentials ≈112 mV/dec, with an exchange current density for the HOR of $\approx 0.36 \times 10^{-3}$ A/cm^{-2}. The (111) surface does not have a transition in the Tafel slope that can be defined in a consistent way, and only one slope of ≈74 mV/dec is observed; the exchange current density for the HOR is $\approx 0.21 \times 10^{-3}$A/cm^{-2}. Note that at low overpotentials all three Pt(*hkl*) surfaces have symmetrical log i *versus* E relationships (inset, Figure 4), indicating that there is a single exchange current density for the hydrogen electrode reaction applicable to both anodic and cathodic processes. It is also important to note that the analysis of the polarization curves recorded for the HOR at higher temperatures (not shown) revealed that the Tafel slopes were directly proportional to the temperature, with the symmetry coefficient, β, for the hydrogen reaction being independent of temperature, see Table 1.

3.2.3. Exchange Current Densities. In the previous sections, we have shown that the kinetics of the hydrogen reaction on Pt(110) is difficult to measure in the Tafel region because of its high exchange current density. However, the same property makes it possible to measure the exchange current density by conducting measurements in the vicinity of the reversible potential, often referred to as the "micropolarization region" or the "linear-current potential" region.[20a] In our work, the polarization curves were analyzed in the micropolarization region (±10 mV), Figure 5, in which a linear relationship

TABLE 1: Kinetic Parameters for the HER and HOR on Pt(*hkl*) in 0.05 M H_2SO_4 at Different temperatures

Pt(*hkl*)	Tafel slope (mV dec^{-1})	exchange current density[a] (mA cm^{-2}) 274 K	303 K	333 K	activation energy (kJ mol^{-1})	mechanism **rds**
Pt(110)	2.3*RT*/2*F*	0.65	0.98	1.35	9.5	**Tafel**−Volmer
Pt(100)	2.3*RT*/3*F*[b]					
	2(2.3*RT*/*F*)[c]	0.36	0.60	0.76	12	**Heyrovsky**−Volmer
Pt(111)	≈2.3*RT*/*F*	0.21	0.45	0.83	18	Tafel−Volmer, Heyrovsky−Volmer

[a] Obtained from a linear polarization method. [b] Low current density. [c] High current density.

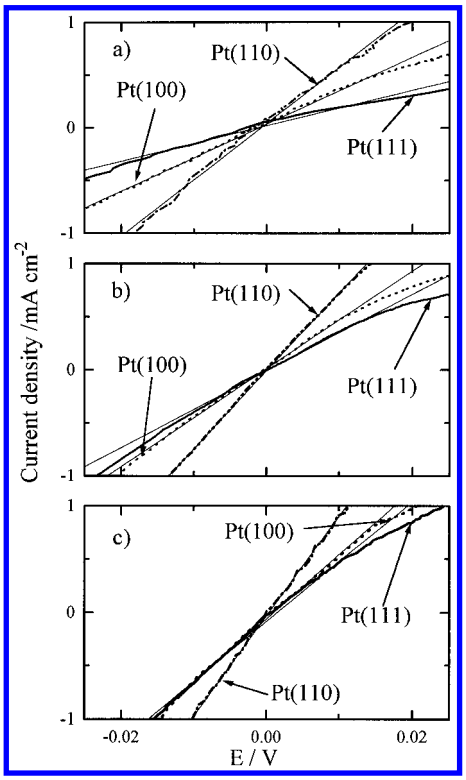

Figure 5. Comparison of polarization curves for the HER and the HOR on Pt(*hkl*) in 0.05 M H_2SO_4 in the "micropolarization" potential region at (a) 274 K, (b) 303 K, and (c) 333 K. Straight lines are the slopes used to obtain the exchange current densities (see text). Rotation rate was 900 rpm and sweep rate 10 mV/s.

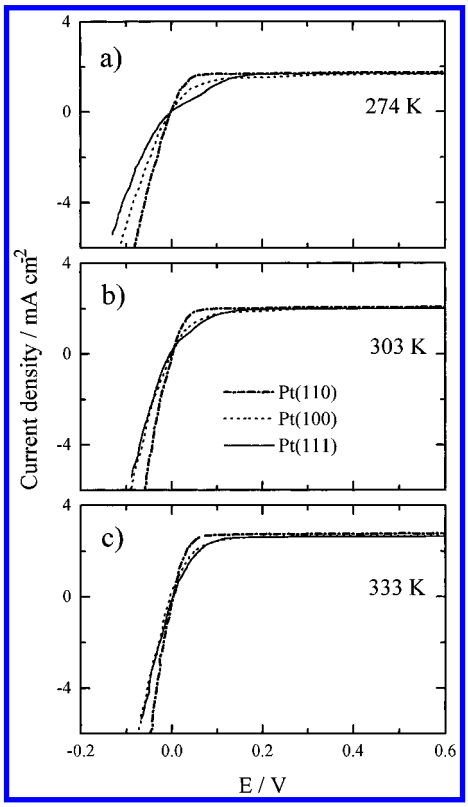

Figure 6. Broad potential range polarization curves for the HER and the HOR on Pt(*hkl*) in 0.05 M H_2SO_4 at (—) 274 K, (- - -) 303 K, and (— —) 333 K; rotation rate, 900 rpm; sweep rate, 10 mV/s.

between the current density and the overpotential is valid; *e.g.*,

$$i = i_o(\eta F/RT) \qquad (3)$$

where i_0 is the exchange current density and η (±10 mV) is the applied overpotential. Figure 5 shows the magnification of currents in the vicinity of the reversible potential. Current *versus* potential data yields straight lines with the slope corresponding to the exchange current density; see Figure 5 and Table 1. While the data in Figure 5 is only for one rotation rate, we note that essentially identical slopes were obtained at all rotation rates used here. Examination of eq 1 reveals that the pure diffusion overpotential will also have a "linear" region, but with a slope proportional to i_d not i_0, and thus would be rotation rate dependent, which these are not. At the same temperature, the exchange current densities increase in the order $i_{0(111)} < i_{0(100)} < i_{0(110)}$, which gives the order of absolute kinetic activities of three surfaces. The values of the exchange current densities determined from the data in Figure 5 are summarized in Table 1. With reference to the anodic Tafel plots in Figure 4, note that for (111) and (100) surfaces the exchange current densities, determined from the slopes in the micropolarization region and those determined by extrapolation from the linear Tafel region, are in excellent agreement (within 5%). This concurrence supports the interpretation of the linear regions of the Tafel plots for these surfaces as true Tafel slopes. For the highly active (110) surface, there is some discrepancy between the exchange current extrapolated from the Tafel plot (0.45 mA cm^{-2}) and that determined from the micropolarization region (0.65 mA cm^{-2}), indicating that the Tafel region for this surface may still contain some diffusional overpotential, *i.e.*, the true kinetic Tafel may be slightly higher than 28 mV/dec, *e.g.*, 30−35 mV/dec.

Anodic and cathodic polarization curves for the different Pt(*hkl*) surfaces are compared at three different temperatures from 274 to 333 K in Figure 6. This comparison clearly shows that the order of activity for the HER and the HOR on Pt(*hkl*) seen at 274 K is maintained at higher temperatures. The exchange current densities determined from the micropolarization data are summarized in Table 1. These results show clearly that, while the structural sensitivity is very pronounced at low temperatures (274−293 K), in the temperature range ≈303−333 K the variation in the kinetics of the hydrogen reaction between crystal faces is less pronounced (especially between the (111) and (100) surfaces). This reconciles, at least in part, the absence of structure sensitivity in all previously published results[6−8] for the HER on Pt(*hkl*) at room temperature. The temperature dependencies of the relative rates of reaction appear to indicate a compensation effect from structure-dependent activation energies, causing this convergence of the kinetics on the different crystal faces of Pt at higher temperatures.

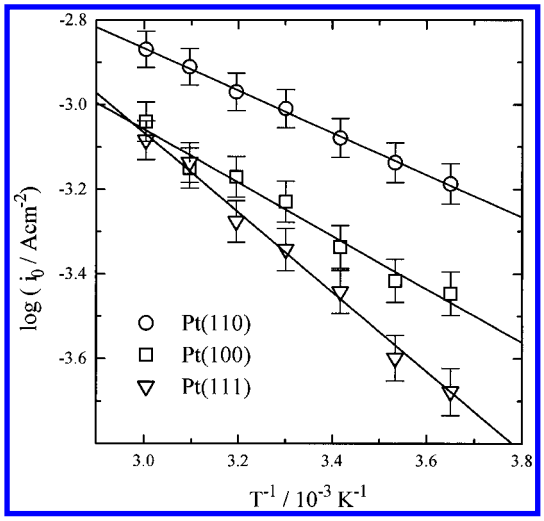

Figure 7. Arrhenius plots of the exchange current densities (i_o) for Pt(*hkl*) over the full range of temperatures employed in this study.

3.2.4. Activation Energies. From Figure 6 it is quite clear that the kinetics of both the HER and the HOR increase significantly by increasing the temperature even in this relatively narrow range of absolute temperature. Qualitatively, the biggest temperature effect is observed at the least active Pt(111) face, with a much smaller temperature effect on the most active surface, Pt(110). Using the values of $i_{0(hkl)}$ determined on Pt(*hkl*) over the temperature range 274−333 K, we have determined the apparent activation energies for the hydrogen reaction on Pt(*hkl*) in 0.05 M H_2SO_4 from the Arrhenius relation

$$\frac{\mathrm{d}\log i_0}{\mathrm{d}(1/T)} = -\frac{\Delta H^{0\#}}{2.3R} \tag{4}$$

where $\Delta H^{0\#}$ is the apparent enthalpy of activation at the reversible potential (from hereafter, activation energies) for the hydrogen reaction on Pt(*hkl*). Arrhenius plots for all three single-crystal surfaces are shown in Figure 7, and the slopes correspond to the activation energies: 9.5 kJ/mol for Pt(110), 12 kJ/mol for Pt(100), and 18 kJ/mol for Pt(111). The fact that the most active surface also has the lowest activation energy is a "classical" result for electrocatalytic reactions and indicates that the energy of adsorption of the reactive intermediate plays the dominant role in the kinetics (*versus* the pre-exponential terms, which contain the coverage factor).[1d]

4. Discussion

The experimental results we have reported in previous sections demonstrate clearly that the kinetics of both the HER and HOR on Pt(*hkl*) in acid solution is a function of the crystallographic symmetry of the platinum surface. We found, *for the first time*, that at the same temperature the exchange current density increases in the order $i^0_{111} < i^0_{100} < i^0_{110}$, which gives the order of the absolute kinetic activities of the three surfaces; Pt(111) < Pt(100) < Pt(110). We also found that every crystal face has a unique Tafel slope for the HOR, and that activation energies for the HER and the HOR decrease in the same sequence, $\Delta H^{\#}_{111} > \Delta H^{\#}_{100} > \Delta H^{\#}_{110}$. In discussion which follows, from these experimentally determined kinetic parameters we will attempt to resolve the molecular-level interactions which control the kinetics of the hydrogen reaction on Pt(*hkl*) in acid solution. The discussion is focused on various possible reactive intermediates, and their role in the mechanism of the hydrogen reaction.

4.1. Mechanism for the HOR and HER in Acid Solution on Pt(*hkl*). The mechanism for the HOR on a polycrystalline platinum electrode in acid electrolytes[21−23] is usually assumed to proceed by an initial adsorption of molecular hydrogen, which involves either slow dissociation of H_2 molecules into the atoms, eq 5, or the ion−atom recombination step, eq 6, followed by

$$H_2 \xrightarrow{\text{rds}} H_{ad} + H_{ad} \tag{5}$$

$$H_2 \xrightarrow{\text{rds}} H^+ + H_{ad} + e^- \tag{6}$$

$$H_{ad} \leftrightarrow H^+ + e^- \tag{7}$$

the fast charge-transfer step, eq 7, *i.e.*, historically refereed to some accounts as the Tafel−Volmer (steps 5 and 7) and Heyrovsky−Volmer (steps 6 and 7) sequences, respectively. If we assume that kinetic parameters, such as the Tafel slopes and the activation energies, are the same for the HOR and HER close to the hydrogen reversible potential, then, at low overpotentials the mechanism for the HER would be the same as that for the HOR, *i.e.*, the first fast charge-transfer step, eq 7, is followed either by the Volmer−Tafel sequence or by the Volmer−Heyrovsky sequence. It is important to note that the adsorbed hydrogen, designated as H_{ad} in eqs 5−7, is *the* reactive intermediate in the HOR and the HER, and therefore, the kinetics of the hydrogen reaction is completely determined by the interaction of H_{ad} with the platinum surface atoms, *e.g.*, the adsorption energy and coverage. Unfortunately, relatively little is known about the nature of H_{ad} on Pt(*hkl*) in electrolytic solutions *at potentials close to the equilibrium potential*. At potentials more positive than *ca*. 0.05 V, there have been extensive studies of the nature of the adsorbed state of hydrogen on Pt (and the Pt group metals). For the purpose of distinguishing the different possible states of adsorbed hydrogen, it is convenient to employ simply a thermodynamic notation, referring to strongly adsorbed states as underpotentially deposited hydrogen, H_{upd}, and to a weakly adsorbed states as the reactive intermediate, H_{ad}, (in Conway notatation: overpotentially deposited hydrogen, H_{opd}). The actual physical state of either H_{upd} or H_{ad} has been and continues to be the subject of intensive study. It is now well-established that H_{upd} is strongly dependent on the crystallographic orientation of the Pt surface,[7] but it is not clear that H_{upd} is the reactive intermediate, H_{ad}, of reactions 5−8. In fact, there are numerous references in the literature[4,5] that H_{ad} is a weakly adsorbed state of hydrogen which becomes populated only at potentials close to the Nernst potential. We had previously proposed[5] for the alkaline electrolyte that the weakly adsorbed state H_{ad} on Pt(*hkl*) is coupled to the strongly adsorbed state of H_{upd} by an as yet uncertain mechanism, so that there is an indirect effect of H_{upd} on the kinetics, with an attendant crystallographic sensitivity. Although the coexistence of H_{upd} and H_{ad} on Pt(*hkl*) over the same potential range has never been proven experimentally in either electrolyte, we propose that H_{upd} plays an important role in the kinetics of the HER and the HOR in the acid solution as well. To understand what this role is, we examine what is known about the nature of H_{upd} on Pt(*hkl*) in acid and whether there is new insight into the nature of the inter-relation of H_{ad} and H_{upd}.

4.1.1. The Nature of the H_{upd} on Pt(*hkl*). The flat shape of the hydrogen peaks in the cyclic voltammogram for the Pt(111) surface is an indication that H_{upd} on Pt(111) obeys the condition in which a strong lateral repulsion exists between the adsorbed species. Consequently, the standard free energy of hydrogen adsorption, $\Delta G°$, should be expected to have a linear decrease in absolute value of $\Delta G°$ on θ[20b]

$$|\Delta G^{\circ}_{\theta}| = |\Delta G^{\circ}_{\theta=0}| - r\theta \tag{8}$$

where $\Delta G^{\circ}_{\theta}$ is the free energy change in the adsorption reaction

$$H^{+} + e^{-} \leftrightarrow H_{upd} \tag{9}$$

and r is the rate of change of free energy of adsorption with H_{upd} coverage. Keeping in mind the relationship between the standard free energy of adsorption and the equilibrium constant for reaction 9, it is very easy to develop an adsorption isotherm which can take into account the variation of the standard free energy of the adsorption of hydrogen with a surface coverage:

$$\left[\frac{\theta}{1-\theta}\right] \exp(r\theta/RT) = K_0 C \exp(EF/RT) \tag{10}$$

This equation is known as the Frumkin isotherm, where K_0 is the equilibrium constant for $\theta = 0$. At intermediate values of the coverage, the pre-exponential term, $\theta/(1-\theta) \approx 1$, varies little with θ compared with the variation of the exponential term, so one can write the Frumkin isotherm in a logarithmic form:

$$\theta = (2.3RT/r) \log(K_0 C) + (F/r)E \tag{11}$$

This equation predicts the linear dependence of θ on E (eq 11 is often referred to as the Temkin isotherm, although Temkin had never used this form[20b]). It can also be seen that $r = 0$ leads to the Langmuir isotherm, *i.e.*, the Langmuir isotherm is a special case of the Frumkin isotherm.

Figure 8 shows numerical values of the fractional coverage $\theta_{H_{upd}}$ *versus* the potential for Pt(111) at 274, 303, and 333 K. We found that the best fit for the hydrogen adsorption on Pt(111) was derived by curve fitting eq 11 using the assumption that ΔG° has a linear decrease in absolute value on $\theta_{H_{upd}}$ (see dotted curves in Figure 8), *i.e.*, from ≈40 kJ/mol at $\theta \approx 0$ mL to ≈12.5 kJ/mol at $\theta \approx 0.66$ mL, shown in Figure 8. The adsorption energies found in this work for H_{upd} on Pt(111) are very close to those reported by Ross.[24a] The best fit values of a parameter $f = r/RT$, which characterize a lateral interaction in two dimensions in the hydrogen adlayer, are very high ($f \approx 15.9-18$ from the temperature range 274−333 K), implying a strong lateral repulsion between H_{upd} on Pt(111).[24b] Unfortunately, because of close coupling of specific anion adsorption with the hydrogen adsorption on Pt(100) and Pt(110), a quantitative study of the hydrogen adsorption cannot be made on these two surfaces in sulfuric acid solution. At the present time we can only speculate about both the change in the free energy of the adsorption with the surface coverage and the energy of interaction between the H_{upd}. On the basis of a fact that a full monolayer of H_{upd} can be adsorbed on Pt(100) and Pt(110), however, it appears reasonable to suggest that the decrease in the heat of adsorption with coverage is much smaller on these two surfaces than on the Pt(111) surface. In fact, we found by surface X-ray scattering (SXS) that the interaction of H_{upd} with Pt(111) is rather weak and H_{upd} is adsorbed *onto* the Pt(111) surface.[15] The same type of SXS experiments indicated that interaction of H_{upd} with the (100) sites is stronger and that close to the monolayer some of the H_{upd} adatoms might sit in deeper potential wells, *e.g.*, the 4-fold hollow sites, and thus be more "in" the surface rather than "on" the surface. In the case of Pt(110) we have recently shown that the most possible sites for the adsorption of hydrogen on Pt(110) are the 3-fold coordinated sites below the top most (110) rows of Pt atoms.[15] There is a pronounced relaxation of the top most atomic rows, which are expanded into the electrolyte with the amount of expansion depending on potential. This may indicate that a significant fraction of H_{upd} is below the surface (subsurface hydrogen), causing expansion of the top most platinum atoms. It should be noted that X-ray scattering measurements are not *directly* sensitive to the location of hydrogen atoms on or below the surface. The X-ray measurements do, however, accurately measure the expansion of the surface platinum atoms as a function of electrode potential.

Recent studies using vibrational spectroscopy provide a mixed picture about the nature of H_{upd} and H_{ad}. Conventional infrared spectra by Ogasawaro and Ito[25] found H−Pt bands indicative of on-top adsorption sites on all three low-index surfaces of Pt(*hkl*), but only at potentials very close to the Nernst potential. There were no band intensities found that were correlated to the coverage by H_{upd}. These results were similar to an earlier report by Bewick and co-workers[26] for polycrystalline Pt. Very different vibrational spectra were reported more recently by Tadjaddine and co-workers[27] using visible−infrared sum frequency generation (SFG) with the free electron laser at Orsay (CLIO). These spectra, which have impressive signal-to-noise ratios, clearly indicate H−Pt bands that correlate with coverage in both the underpotential deposition and HER overpotential region. The frequencies of the bands in the underpotential deposition region are reported to correspond to terminally bonded hydrogen, *i.e.*, on-top sites, while in the overpotential region a new band appears that is assigned to a dihydride configuration, H_2−Pt. The latter is suggested to be the active intermediate, H_{ad}, in the HER, but this state was not detectable at +0.05 V. Tadjaddine and co-workers did not find any bands at low frequency, characteristic of multiply bonded H−Pt, *e.g.*, in 3-fold or 4-fold hollow sites, such as is seen for H−Pt in ultra high vacuum, and which we had proposed above for H_{upd}. It may be that the inference we have drawn from the surface relaxation measurements is not correct, that relaxation is not a consequence of H_{upd} in or below the surface, but is a consequence of other more complex interactions.

In the following, we present an analysis of the kinetics in terms of the same structural models for the H_{upd} as we used previously with alkaline solution and rationalize its role in the rate determining step (rds) and in the resulting structure sensitivity of the reaction. There are two modes of action of H_{upd} on the kinetics of the HER and the HOR on Pt(*hkl*) in 0.05 M H_2SO_4 which we considered: H_{upd} adatoms block the adsorption of the active intermediate H_{ad}, *i.e.*, they compete for the same site, and/or affect the adsorption energy of H_{ad} on the bare Pt sites which are neighbored by the H_{upd}.

4.1.2. Mechanism of the HER and the HOR on Pt(110). Assuming that the sites for the adsorption of H_{upd} on Pt(110) are the 3-fold coordinated sites below the top most rows of Pt atoms and that the significant amount of H_{upd} may be below the surface (subsurface hydrogen), H_{upd} on Pt(110) is most probably a spectator during the hydrogen reaction. In the absence of more definitive information about the state of H_{ad}, the model that appears to rationalize the results for the HOR at low anodic overpotentials on Pt(110) is one which follows application of the Langmuir (ideal) adsorption isotherm of H_{ad} and the ideal dual-site form of the Tafel−Volmer sequence.[1a] The Tafel relationship observed for Pt(110) over two decades of current density for the HOR at low overpotentials with a slope $\approx 2.3RT/2F$ (Figure 4 and Table 1), clearly indicates that the atom−atom recombination step is indeed the rds. Considering that an activation energy of ≈9.5 kJ/mol is reasonable for a reaction like the atom−atom recombination step under Langmuirian conditions, we can propose that the HOR on Pt(110) proceeds by the Tafel−Volmer sequence, the atom−atom recombination step being the rds. Assuming that on either

side of the equilibrium potential for the hydrogen reaction the (110) surface always provides the same number of active centers (pair of Pt top-sites), then the kinetics and the mechanism of the HER and HOR should be the same, as confirmed from the symmetrical shape of the polarization curves in the inset of Figure 4, and by the fact that the same values for the exchange current densities are observed for the HER and HOR. Thus, in the HER on Pt(110) in sulfuric acid, a fast charge-transfer reaction is followed by rate-controlling atom−atom recombination step (Volmer−Tafel sequence).

4.1.3. Mechanism of the HER and the HOR on Pt(100). The adsorption isotherm Figure 2 shows that the HOR on Pt(100) occurs on the surface which is "fully" covered by H_{upd}, as it was for the HOR on Pt(110). Note that, even when Pt(110)-(1 × 2) is "fully" covered by H_{upd}, the top rows of platinum atoms are still unoccupied and available for the adsorption of H_{ad}, *e.g.*, as terminally bonded H−Pt. In contrast, on the geometrically homogeneous Pt(100)-(1 × 1) surface, if there is only one type of site for hydrogen adsorption, then a (100) surface covered by 1 mL of H_{upd} should be completely inactive for the HOR because the platinum sites are completely blocked by H_{upd}. A comparison of the anodic part of the polarization curves in Figure 3 with the underpotential deposition of hydrogen in Figure 2 clearly shows that the HOR indeed takes place on Pt(100) fully blocked by the inactive H_{upd} adatoms. The implication is that unoccupied Pt sites, required for the adsorption of H_{ad}, can only be created if some amount (unknown) of the H_{upd} adatoms sit in deeper potential wells on the surface, e.g. the 4-fold hollow sites, freeing top-sites, neighbored by subsurface H_{upd}, to serve as adsorption centers for H_{ad}. Although the number of on-top active sites near 0 V is unknown, we propose that this number is relatively small, and that the Pt(100) is active for the HER at low overpotentials only due to a very high turnover rate at these sites. A small number of active centers for the H_{ad} adsorption would greatly reduce the number of pair-sites which are required for the chemical recombination step to occur. Consequently, the preferred reaction pathway on Pt(100) at low overpotential maybe one which requires only one active site in the rds, like the ion−atom recombination reaction. In fact, an activation energy of ≈12 kJ/mol for the HER and the HOR found at the hydrogen reversible potential, and two separate Tafel regions, 2.3*RT*/3*F* at low current densities and 2.3*RT*/*F* at higher current densities, found for the HOR strongly imply that the reaction mechanism is indeed different on Pt(100) than on Pt(110). On the basis of these Tafel slopes and this model of H_{ad}, we propose that the mechanism for the HOR on the Pt(100) proceeds through the ideal Heyrovsky−Volmer sequence with the ion−atom reaction as the rds (see Gileadi[20b] for the case of small coverage by H_{ad} at low overpotentials and "maximum" surface coverage by H_{ad} at high overpotentials). As in the case of Pt(110), the anodic/cathodic symmetry for the polarization curves for the (100) surface, see inset of Figure 4, can be rationalized as arising from the same mechanism in both overpotential regions, *i.e.*, the HER follows the Volmer−Heyrvsky sequence.

4.1.4. Mechanism of the HER and the HOR on Pt(111). The influence of H_{upd} on the kinetics of HOR is most pronounced for the Pt(111) surface, as one can see by comparing Figures 2 and 4. On Pt(111), the onset of the HOR appears to be correlated with the desorption of H_{upd}, which suggests that the HOR mechanism on Pt(111) at low overpotentials follows a dual-site pathway, the Tafel−Volmer sequence. The relatively high activation energy for the hydrogen reaction on Pt(111), ≈18 kJ/mol, that almost doubled *versus* the same reaction

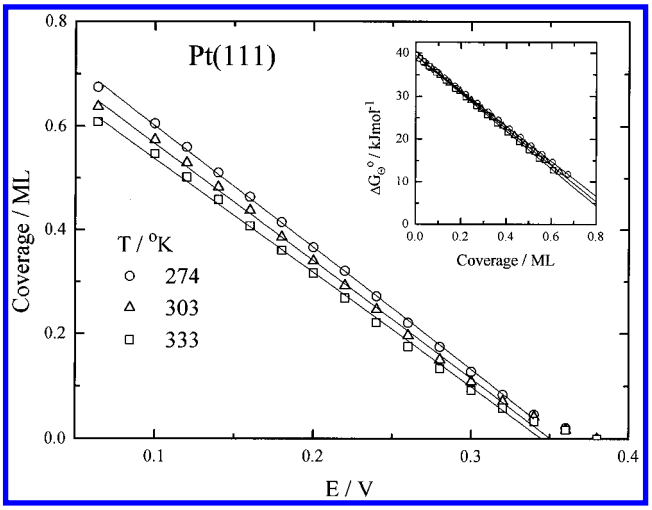

Figure 8. Adsorption isotherms for H_{upd} on Pt(111) in 0.05 M H_2SO_4 at 274 K, 303 K, and 333 K. Inset. Change of the free energy of adsorption of the H_{upd} with surface coverage of H_{upd}, obtained by fitting the coverage data with the Frumkin isotherm (eq 10).

pathway on Pt(110) may be due to the strong repulsive interaction between H_{ad} adatoms, which is indicated by the adsorption isotherm of H_{upd} in Figure 8. It was hoped that the reaction mechanism of the HOR would be resolved in a definitive way by the analyzing the Tafel slopes, as we did for the Pt(110) and Pt(100). Unfortunately, this does not appear to be possible at this time, principally because the Tafel slope of ≈74 mV/dec at 274 K obtained for the HOR at Pt(111) cannot be interpreted unambiguously. A Tafel slope of ≈2.3*RT*/*F*, obtained over the entire temperature range studied in this work, implies that the adsorption of the reaction intermediates on Pt(111), H_{ad}, does not follow Langmuirian conditions. Actually, we noted earlier that the equilibrium constant for the underpotential deposition of hydrogen on Pt(111) is an exponential function of H_{upd} coverage and follows the Frumkin isotherm, eq 11. If H_{ad} simply follows a Frumkin isotherm, then, assuming the rate-determining step is either the atom−atom recombination step or atom−ion recombination step, it will yield the same slope of 2.3 *RT*/*F*. Even if H_{upd} is not the active intermediate in the HOR and the HER, H_{upd} could still have a significant indirect effect on the kinetics on the HER and the HOR on Pt(111). H_{upd} may alter both the electronic properties of the Pt substrate and/or the interaction of H_{ad} with the surface, but the number of mathematical models for such effects is arbitrarily large in the absence of other knowledge.

5. Conclusions

The hydrogen evolution (HER) and the hydrogen oxidation reactions (HOR) were studied on platinum single crystals in a sulfuric acid solution over the temperature range 274−333 K. We found, for the first time, that at the same temperature the exchange current density for the hydrogen reaction increases in the order $i^0_{111} < i^0_{100} < i^0_{110}$, which gives the order of absolute kinetic activities of Pt(*hkl*), Pt(111) < Pt(100) < Pt(110). We also found that every crystal face has an unique, ideally temperature-dependent, Tafel slope for the HOR: a single slope of 2.3*RT*/2*F* and 2.3*RT*/*F* on Pt(110) and Pt(111), respectively; and two slopes, 2(2.3*RT*)/3*F* at low current densities and 2(2.3*RT*)/*F* at high current densities on Pt(100). The activation energies for the HER and the HOR decrease in the sequence $\Delta H^{\#}_{111} > \Delta H^{\#}_{100} > \Delta H^{\#}_{110}$, and the structure sensitivity of the kinetics is directly related to these differences in activation energy. These differences in activation energy with the crystal

face are attributed to structure-sensitive heats of adsorption of the active intermediate, H_{ad}, whose physical state is unclear. We analyzed the kinetic data with a model for the coupling of this unknown state H_{ad} with the well-known adsorbed state of hydrogen, H_{upd}, whose adsorption energy is strongly structure-sensitive. On both the (110) and (100), we assumed an indirect effect of H_{upd} on H_{ad}, which are distinctly different species. The reaction intermediate, H_{ad}, was assumed to follow Langmuirian isotherms on these surfaces. We concluded that on Pt(110) the reaction proceeds through the Tafel−Volmer sequence with the atom−atom recombination step (Tafel) as the rds. On Pt(100), the ion−atom reaction (Heyrovski) controls the rate of the reaction in the Heyrovsky−Volmer sequence. In the case of Pt(111), we found that energy of adsorption of H_{upd} has a linear decrease with coverage, from ≈40 kJ/mol at $\theta \approx 0$ mL to ≈12.5 kJ/mol at $\theta \approx 0.66$ mL, which is well-fit by a Frumkin isotherm. The best fit values of a parameter $f = r/RT$ ($f \approx 15.9-18$ from the temperature range 274−333 K) correspond to a strong lateral repulsive interaction in the hydrogen adlayer on Pt(111). We concluded that this strong repulsive interaction is the cause of the relatively high activation energy on this surface and consequently the lowest activity of the three crystal faces. The reaction mechanism on Pt(111) could not, however, be resolved in a definitive way.

Acknowledgment. This work was supported by the Assistant Secretary for Conservation and Renewable Energy, Office of Transportation Technologies, Electric and Hybrid Propulsion Division of the U.S. Department of Energy under contract number DE-AC03-76SF00098.

References and Notes

(1) See, for example: (a) Vetter, K. J. *Electrochemical Kinetics*; Bruckensein, S., Howard, B., Trans. Eds.; Academic Press: New York, 1967; pp 516−614. See pages 550-1 for a complete historical account. (b) Bockris, J. O'M.; Ready, A. K. *Modern Electrochemistry*; Plenum Press: New York, 1983; Vol. 2. (c) Conway, B. E.; Bockris, J. O'M. *J. Chem. Phys*. **1957**, *26*, 532. (d) Parsons, R. *Trans. Faraday Soc*. **1958**, *54*, 1053. Gerisher, H. *Bull. Soc. Chim. Belg*. **1958**, *67*, 506. (e) Krishtalik, L. I. In *Advances in Electrochemistry and Electrochemical Engineering*; Delahay, P., Tobias, C. W., Eds.; John Wiley & Sons: New York, 1970; Vol. 7. (f) Trasatti, S. In *Advances in Electrochemistry and Electrochemical Engineering*; Gerisher, H., Tobias, C. W., Eds.; John Wiley & Sons: New York, 1977; Vol. 10. (g) Lasia, A. *Curr. Top. Electrochem*. **1993**, *2*, 239.

(2) Physhnogreva, I. I.; Skundin, A. M.; Vasiliev, Yu. B.; Bagotski, V. S. *Elektrokhimiya* **1970**, *6*, 142.

(3) Schulander, S.; Rosen, M.; Flinn, D. *J. Electrochem. Soc.* **1970**, *117*, 1251.

(4) Protopopoff, E.; Marcus, P. *J. Chim. Phys.* **1991**, *88*, 1423.

(5) Marković, N. M.; Sarraf, T. S.; Gasteiger, H. A.; Ross, P. N. *J. Chem. Soc., Faraday Trans.* **1996**, *92*, 3719 and references therein.

(6) (a) Seto, K.; Iannello, A.; Love, B.; Lipkowski, J. *J. Electroanal. Chem.* **1987**, *226*, 351.

(7) Kita, H.; Ye, S.; Gao, Y. *J. Electroanal. Chem.* **1992**, *334*, 351.

(8) Gomez, R.; Fernandez-Vega, A.; Felui, J. M.; Aldaz, A. *J. Phys Chem.* **1993**, *97*, 4769.

(9) For example, see: Clavilier, J.; Rodes, A.; El Achi, K.; Zamakhchari, M. A. *J. Chim. Phys.* **1991**, *88*, 1291 and references therein.

(10) Bagotzky, V. S.; Osetrova, V. *J. Electroanal. Chem.* **1973**, *43*, 233.

(11) Marković, N. M.; Gasteiger, H. A.; Ross, P. N. *J. Phys Chem.* **1995**, *99*, 3411.

(12) See, for example: (a) Al-Jaaf-Golze; Kolb, D. M.; Scherson, D. *J. Electroanal. Chem.* **1986**, *200*, 353. (b) Wagner, F. T.; Ross, P. N. *J. Electroanal. Chem.* **1988**, *250*, 301. (c) Marković, N. M.; Marinković, N. S.; Adzić, R. R. *J. Electroanal. Chem.* **1988**, *241*, 309. (d) Orts, J. M.; Gomez, R.; Feliu, J. M.; Aldaz, A.; Clavilier, J. *Electrochim Acta* **1995**, *39*, 1519. (e) Savich, W.; Sun, S. G.; Lipkowski, J.; Wieckowski, A. *J. Electroanal. Chem.* **1995**, *388*, 233.

(13) Marković, N. M.; Grgur, B. N.; Lucas, C. A.; Ross, P. N. *Surf. Sci.*, in press.

(14) Tidswell, I. M.; Marković, N. M.; Ross, P. N. *Phys. Rev. Lett.* **1993**, *71*, 1601.

(15) (a) Tidswell, I. M.; Marković, N. M.; Ross, P. N. *J. Electroanal. Chem.* **1994**, *376*, 119. (b) Lucas, C. A.; Marković, N. M.; Ross, P. N. *Phys. Rev. Lett.* **1996**, *77*, 4922.

(16) Zolfaghari, A.; Jerkiewicz, G.; Sung, Y. E.; Wieckowski, A. In *Proceedings of the Sixth International Symposium on Electrode Processes*; The Electrochemical Soc. Inc.: Pennington, NJ, 1996; pp 150.

(17) Morin, S.; Dumont, H.; Conway, B. E. *J. Electroanal. Chem.* **1996**, *412*, 39.

(18) Gasteiger, H. A.; Marković, N. M.; Ross, P. N. *J. Phys Chem.* **1995**, *99*, 8290.

(19) Marković, N. M.; Ross, P. N. *J. Electroanal. Chem.* **1992**, *330*, 499 and references therein.

(20) Gileadi, E. *Electrode Kinetics for Chemical Engineers and Materials Scientists*; VCH Publishers (UK): Cambridge, 1993; pp 116, 261−280.

(21) Ludwig, F.; Sen, R. K.; Yeager, E. *Electrochemiya* **1967**, *13*, 847.

(22) Conway, B. E.; Bai, L. *J. Electroanal. Chem.* **1986**, *198*, 149.

(23) Bai, L.; Harrington, D. A.; Conway, B. E. *Electrochim. Acta* **1987**, *32*, 1713.

(24) (a) Ross, P. N. *Surf. Sci*. **1981**, *102*, 463. (b)Marinković, N. S.; Marković, N. M.; Adzić, R. R. *J. Electroanal. Chem.* **1992**, *330*, 434.

(25) Ogasawara, H.; Ito, M. *Chem. Phys. Lett.* **1994**, *221*, 213.

(26) Bewick, A.; Russell, J. W. *J. Electroanal. Chem*. **1982**, *132*, 329.

(27) Tadjaddine, A.; Peremans, A. *J. Electroanal. Chem.* **1996**, *409*, 115. Tadjaddine, A.; Peremans, A.; Guyot-Sionnest *Surf. Sci*. **1995**, *335*, 210. Peremans, A.; Tadjaddine, A. *J. Chem. Phys.* **1995**, *103*, 7197. Peremans, A.; Tadjaddine, A. *Phys. Rev. Lett*. **1994**, *73*, 3010.